Pure & Appl. Chem., Vol. 65, No. 2, pp. 259–267, 1993.
Printed in Great Britain.

Simulation of simple heterogeneous combustion systems

Ulrich Maas and Jürgen Warnatz

Institut für Technische Verbrennung, Universität Stuttgart, 7000 Stuttgart 80, Germany

Abstract

Two simple heterogeneous combustion processes (droplet combustion and catalytic combustion) are considered, including detailed chemistry in each case:

Droplet Combustion: A numerical study describing the heating, vaporization, and combustion process of a methanol droplet in quiescent air is presented, using a spatially one-dimensional spherical model. Temperature- and pressure dependent properties of the liquid and the gas have been employed in combination with a detailed chemical reaction mechanism in the gas phase. The conservation equations (formulated separately inside the droplet and in its environment) are connected by interface equations and are solved simultaneously. The interface equations account for heat transfer across the droplet boundary, vaporization, and the resulting change of droplet size and boundary temperature. Calculations have been performed for a high pressure and temperature environment and include studies of droplet lifetime, ignition, and the development of temperature profiles in the droplet.

Catalytic Combustion: Some new computational tools have been developed that provide opportunities to analyse the elementary chemical processes that occur at gas-surface interfaces, and couple them to the surrounding fluid flow and to detailed gas phase reaction mechanisms to get a quantitative understanding of catalytic combustion. Using computational methods, the catalysed combustion of lean hydrogen-oxygen mixtures in a stagnation flow over a platinum surface and in a flat-plate boundary layer are considered. Results of the models are compared to two sets of experiments that determine (a) catalytic combustion and ignition limits in hydrogen-oxygen mixtures at low pressure (100 mTorr) and (b) OH concentration profiles in catalytically supported combustion at atmospheric pressure.

1. INTRODUCTION

The success in laminar flame calculations during the last decade has shown that an adequate knowledge of the underlying physical and chemical processes exists. Together with new numerical methods for the solution of large stiff partial differential equation systems, reliable simulations of laminar combustion processes are now possible, based on detailed chemical reaction mechanisms and multicomponent transport models [1-4]. Recently the detailed simulation of heterogeneous combustion processes has gained much interest. Principle aim is to couple the detailed models for the gas-phase processes with a detailed description of physical and chemical processes occurring at surfaces, which play an important role e.g. in droplet combustion, catalytic combustion, coal combustion, etc. Two simple heterogeneous combustion processes (droplet combustion and catalytic combustion) are considered here, including detailed chemistry in each case.

2. DROPLET COMBUSTION

2.1. Introduction

The heating, vaporization and combustion processes of fuel droplets has been an object of intensive research (see e.g. [5-11]). The progress in the field of detailed mathematical modelling now allows to take into account the detailed physical and chemical processes in the droplet as well as at the gas-liquid interface and in the gas-phase. The model presented below describes the combustion of a methanol droplet in quiescent air, considering a high temperature and high pressure environment (i.e. under engine conditions). The combustion, which occurs in the gas-phase, is described by a detailed reaction mechanism. The mathematical model consists of the conservation equations for the liquid and the gas phase and the interface equations which include the interactions between both phases. In order to allow a reliable simulation, the conservation equations for the liquid and the gas phases are solved simultaneously. Boundary conditions at the interface account for heat conduction, vapour pressure, enthalpy of vaporization, diffusion and convection. For the numerical solution a time dependent, one-dimensional spherical model has been employed. Gradient dependent static regridding is used in order to minimize discretization errors (see [10,11] for details).

2.2. Mathematical model

The combustion of single spherical droplet can be simulated for a one-dimensional spherical geometry by solving the conservation equations for mass, species mass, momentum and energy in the droplet and the gas-phase together with the boundary equations at the interface. In the gas-phase convection, caused by the inflow of fuel vapour into the gas phase has to be considered. Therefore, a modified Lagrangian transformation is used, which fixes the origin of the Lagrangian coordinate system to the droplet surface [11]. Together with the transformation equation (1), the partial differential equation system describing the processes in the gas-phase reads [10-12]:

$$\left(\frac{\partial \psi}{\partial r}\right)_t = \rho r^2, \tag{1}$$

$$\frac{\partial \rho}{\partial t} + \rho^2 \frac{\partial \left(v r^2\right)}{\partial \psi} + z_I \frac{r_I^2}{r^2} \frac{1}{\left(\frac{\partial r}{\partial \psi}\right)} \cdot \frac{\partial \rho}{\partial \psi} = 0, \tag{2}$$

$$\frac{\partial v}{\partial t} + r^2 \frac{\partial p}{\partial \psi} - \frac{4}{3} r^2 \frac{\partial}{\partial \psi}\left(\rho \mu \frac{\partial}{\partial \psi}\left(v r^2\right)\right) + 4 r^2 \frac{v}{r} \frac{\partial \mu}{\partial \psi} + z_I \frac{r_I^2}{r^2} \frac{1}{\left(\frac{\partial r}{\partial \psi}\right)} \cdot \frac{\partial v}{\partial \psi} = 0, \tag{3}$$

$$\frac{\partial T}{\partial t} - \frac{1}{\rho c_p} \frac{\partial p}{\partial t} - \frac{1}{c_p} \frac{\partial}{\partial \psi}\left(\rho r^4 \lambda \frac{\partial T}{\partial \psi}\right) - \frac{r^2}{c_p} \sum_{i=1}^{n_s} \rho r^2 \left(\rho D_i^D \frac{w_i}{x_i} \frac{\partial x_i}{\partial \psi} + \frac{D_i^T}{T} \frac{\partial T}{\partial \psi}\right) c_{pi} \frac{\partial T}{\partial \psi}$$

$$+ \frac{1}{\rho c_p} \sum_{i=1}^{n_s} \dot{\omega}_i h_i M_i - \frac{4 \rho \mu}{3 c_p} \left(\frac{\partial \rho v r^2}{\partial \psi}\right)^2 + \frac{4 \mu}{c_p} \frac{\partial}{\partial \psi}\left(v^2 r\right) + z_I \frac{r_I^2}{r^2} \frac{1}{\left(\frac{\partial r}{\partial \psi}\right)} \cdot \frac{\partial T}{\partial \psi} = 0, \tag{4}$$

$$\frac{\partial w_i}{\partial t} - \frac{\partial}{\partial \psi}\left(\rho r^4 \left(\rho D_i^D \frac{w_i}{x_i} \frac{\partial x_i}{\partial \psi} + \frac{D_i^T}{T} \frac{\partial T}{\partial \psi}\right)\right) - \frac{\dot{\omega}_i M_i}{\rho} + z_I \frac{r_I^2}{r^2} \left(\frac{\partial r}{\partial \psi}\right)^{-1} \cdot \frac{\partial w_i}{\partial \psi} = 0, \tag{5}$$

$$p - \frac{\rho R T}{\overline{M}} = 0. \tag{6}$$

In these equations the time t and the Lagrangian coordinate ψ are the independent, the radius r, the density ρ, the velocity v, the temperature T, the mass fractions w_i, and the pressure p the dependent variables. The ideal gas law (6) is used to close the equation system. Furthermore, $\overline{M}$ = mean molar mass of the mixture, R = universal gas constant, z_I = absolute velocity at the interface, r_I = droplet radius, c_p = heat capacity at constant pressure, λ = heat capacity of the mixture, M_i = molar mass of species i, D_i^D = diffusion coefficient of species i into the mixture, D_i^T = thermal diffusion coefficient of the species i, n_s = number of species, x_i = mole fraction of species i, $\dot{\omega}_i$ = molar scale rate of formation of species i, h_i = specific enthalpy of species i, μ = viscosity of the mixture.

The model is able to account for multicomponent droplets [12], for simplicity a one component droplet at spatially constant pressure shall be considered here. In this case the conservation equations in the droplet are reduced to the Lagrangian transformation equation and the conservation equation for energy inside the liquid (index L).

$$\left(\frac{\partial \psi_L}{\partial r_L}\right)_t = \rho_L {r_L}^2 \tag{7}$$

$$\frac{\partial T_L}{\partial t} - \frac{1}{\rho c_{pL}} \frac{\partial p_L}{\partial t} - \frac{1}{c_{pL}} \frac{\partial}{\partial \psi_L}\left(\rho {r_L}^4 \lambda_L \frac{\partial T_L}{\partial \psi_L}\right) = 0 \tag{8}$$

At the interface (index I)boundary equations for the conservation equations need to be formulated. The droplet radius changes according to

$$\frac{\partial r}{\partial t} = -\dot{m} \cdot \frac{M_F}{\rho_{IL}} \qquad \dot{m} = \left(\rho_{F,vap} - \rho_{F,cond}\right) \cdot \frac{u}{M_F} \tag{9}$$

where $\dot{m}$ is the molar flux across the interface, u the temperature dependent velocity of the molecules of the fuel vapour, M_F the molar mass of the fuel, and ρ_{Fvap} and ρ_{Fcond} the densities of vaporizing and condensing fuel, respectively. The indices F, *vap*, *cond* denote the fuel, vaporization and condensation. The balance of the energy flux across the interface, consisting of gas and liquid heat conduction, and enthalpy of vaporization E_{vap}, determines the interface temperature:

$$\lambda_{IL}\left(\frac{\partial T}{\partial r}\right)_L + \lambda_{IG}\left(\frac{\partial T}{\partial r}\right)_G + \dot{m} \frac{E_{vap}}{M_F} = 0. \tag{10}$$

In order to allow a detailed description of the droplet and the interface, temperature dependent properties such as density, heat conductivity, heat capacity, enthalpy, enthalpy of vaporization, surface tension of the liquid, etc. [13] have been used. Further details can be found in [10-12]. The gas phase reaction mechanism used for the simulation of the combustion of a methanol droplet consists of 18 species and 70 elementary reactions [10]. Furthermore, a multicomponent transport model based on the Curtiss Hirschfelder assumption is used for the gas phase[14,15].

For the numerical solution the governing equations are spatially discretized using a radial grid with a non-uniform grid point distribution. The resulting algebraic/ordinary differential equation system is solved by implicit methods (see [10,11] for details).

2.3. Results and discussion

Calculations have been performed for a liquid methanol droplet with an initial temperature of 350K [11]. Time dependent simulations have been carried out for various gas phase temperatures, initial droplet sizes, and different degrees of premixedness of the gas phase with fuel vapour [10-12]. In general, the overall combustion process is governed by three different processes, namely heating of the liquid, vaporization, and, depending on the initial conditions, ignition and combustion of the gas phase. Heating of the droplet is controlled by heat conductivity and heat capacity in the liquid. Vaporization is governed by the vaporization and diffusion of the fuel vapour into the gas phase. Ignition and combustion are determined mainly by the gas phase processes. However, the strong interdependence of all three processes requires a detailed physical and chemical model which couples all the physical and chemical processes.

A typical simulation of an ignition of a droplet shall be described here using a methanol droplet in hot air as an example. We consider a droplet with an initial radius of 25 µm and a uniform temperature of 350K, which is surrounded by air (1100K) at a pressure of 30 bar. The simulation is performed for the whole life time of the droplet and describes the processes taking place in the droplet as well as in the gas phase [11].

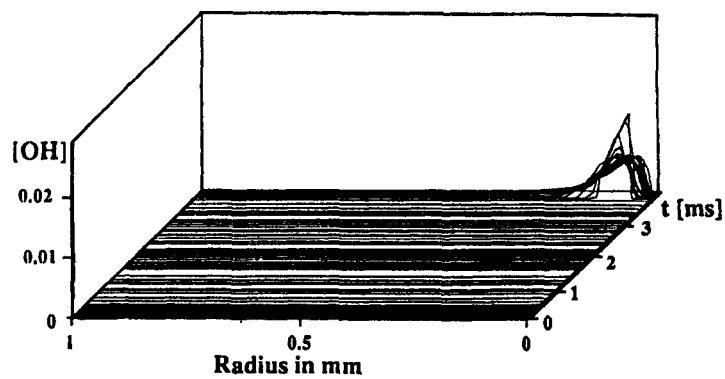

Figure 1: Profiles of temperature during the combustion of a methanol droplet (r_0 = 25 µm, T_0 = 350 K) in air (T_0 = 1100 K, p = 30 bar) [11]

Figure 1 shows the development of the temperature in the gas-phase with time. The droplet is located at the right boundary. Due to the heating of the droplet energy is removed from the gas-phase and the temperature near the interaface is decreased. Vaporization of methanol and subsequent transport into the surrounding air by convection and diffusion cause the formation of a combustible mixture and after about 3.5 ms ignition and flame propagation takes place. The onset of ignition can be seen in a plot of the OH-radical mass fractions (Fig.2), where the exponential increase of the radical pool characterizes the ignition.

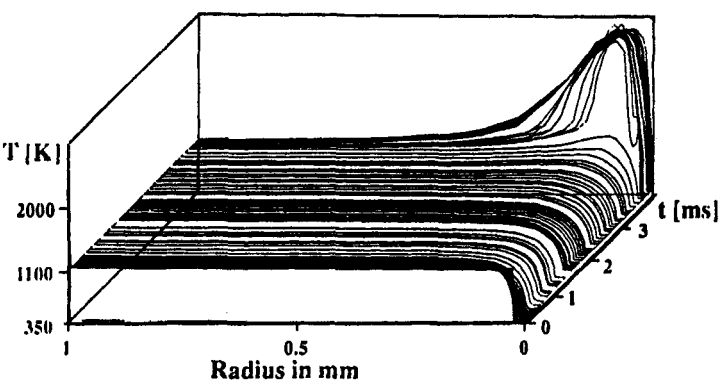

Figure 2: Profiles of hydroxy radical mass fractions during the combustion of a methanol droplet (r_0 = 25 µm, T_0 = 350 K) in air (T_0 = 1100 K, p = 30 bar) [11]

The overall process can be described by the temperature change with time at the centre of the droplet and at the interface as well as by the change of the droplet radius. Figure 3 (left) shows three stages of the droplet combustion: Heating of the droplet without significant vapourization, vaporization, and finally ignition. On the right side of Fig.3 the first stage (namely the heating of the droplet) is shown in detail for a small time interval. At the beginning most of the heat transferred from the hot gas into the droplet is used for heating the droplet rather than for vaporization. This can be seen from the fact that the droplet barely decreases in size. Subsequently the interior of the droplet is heated by heat conduction while simultaneously the radius of the droplet decreases strongly due to vaporization. This process proceeds until the temperature distribution within the droplet is almost uniform.

Subsequently vaporization of the droplet starts. The decrease of the droplet radius in this stage follows a d^2 law. Due to diffusion of fuel vapour into the air a combustible mixture is formed and ignition takes place. The energy released during the ignition process causes the droplet to heat again like in the first stage of the overall process. Then (cf. Fig. 3) the increased interface temperature accelerates vaporization, and a diffusion flame is established around stoichiometry. Furthermore it can be seen, regarding the change in droplet radius, that a detailed calculation of interface processes results in a decrease of droplet size according to the d^2 - law (cf. [5,6,8,9]) during part of the droplet life time. However, physical processes like heating of the droplet due to combustion of the vapour cause the change of the droplet radius to have a much more complicated time depence than a simplified d^2 law can account for (see Fig. 3).

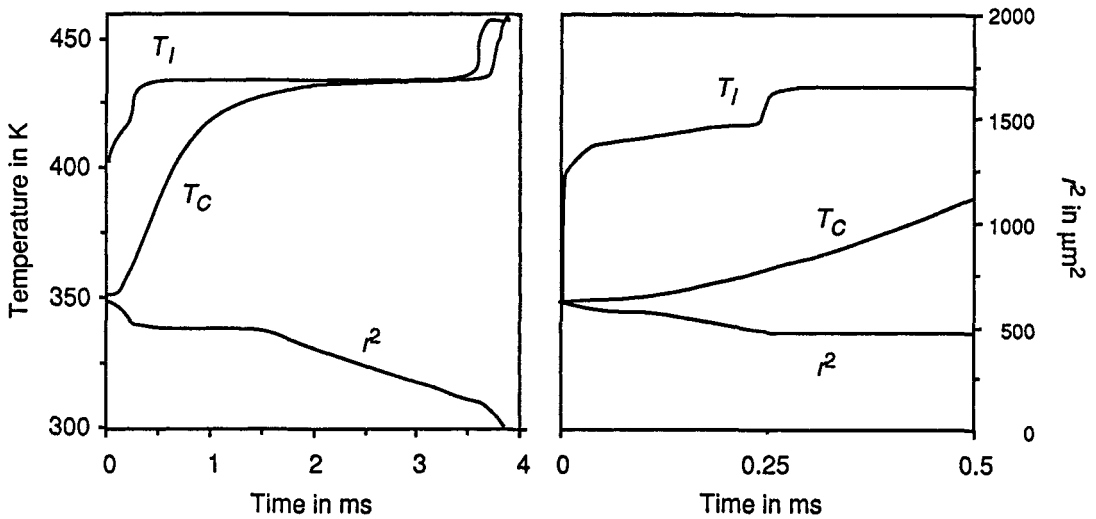

Figure 3: Overall process (left) and droplet heating (right) of a methanol droplet ($r_0 = 25$ µm, $T_0 = 350$ K) in air ($T_0 = 1100$ K, p = 30 bar). Plotted are the temperature in the center of the droplet T_C and at the interface T_l as well as the square of the droplet radius

The calculations performed for the combustion of a single droplet show the strong interdependence of the liquid and the gas phase. Therefore, a detailed understanding of this process requires an as accurate as possible formulation of the interface equations, which has to include the physical interactions of liquid and gas without imposing empirical laws. The results presented show exemplarily the heating of the liquid, its vaporization and the gas temperature development including ignition, during the droplet life time. A variation of initial conditions, as gas phase temperature, droplet size, and degree of premixedness of the gas phase with fuel vapour points out their influence on the droplet life time, the temperature of the liquid, and the ignition limits [12].

3. CATALYTIC COMBUSTION

3.1. Introduction

Catalytic combustion has been known for more than 150 years [16], when *Davy* detected the ability of platinum surfaces to cause combustion of flammable mixtures "without flames," and catalytic combustion of hydrogen has been known since the famous work of *Langmuir* [17]. Nevertheless, there was inadequate quantitative knowledge of this process until recently, when studies of OH desorption from platinum catalysts were carried out using laser-induced fluorescence, LIF (see e. g. [18,19]), leading to some detailed insight into the surface oxidation mechanism of hydrogen which will be necessary in subsequent analysis of hydrocarbon catalytic combustion (experimental results presented e. g. in [20,21]).

Catalytic combustion has a number of potentially important and practical applications like super-lean NO_x-free combustion and generation of low-temperature process heat. Quantitative simulation capabilities can play an important role in accelerating the development in this field. Recently developed computational tools [22-25] provide opportunities to analyse the elementary chemical processes that occur at gas-surface interfaces, and couple them to the surrounding fluid flow and to detailed gas phase reaction mechanisms.

The stagnation flow field and the flat-plate boundary layer are particularly amenable to analysis and to experimental investigation. The two-dimensional flow fields can be reduced to one-dimensional situations by a boundary layer or a similarity transformation. Furthermore, there are measurements available for these configurations, i. e. experiments of *Ljungström et al.* in a stagnation flow field [18] and of *Cattolica and Schefer* in a flat-plate boundary layer [26,27], which are accompanied by computations with a detailed gas-phase reaction mechanism (but global surface chemistry).

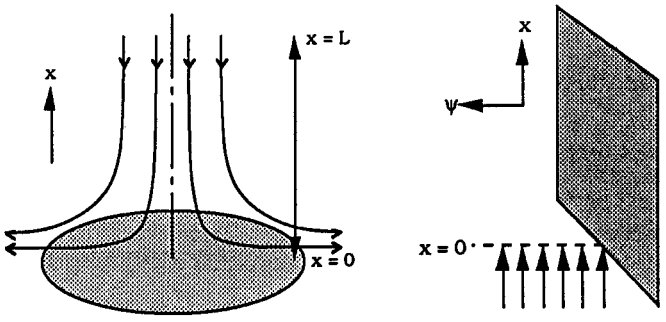

Figure 4. Sketch of a stagnation flow field and a flat plate boundary layer

3.2. Mathematical model

3.2.1. Stagnation-flow field

The stagnation-flow field is shown graphically in Fig. 4. At a distance of $x=L$ above a flat plate a uniform (independent of radius) downward velocity is imposed. In addition, the gas composition and temperature are also independent of radius and the radial velocity component is zero. By confining our attention to the centre portions of the surface edge effects can be neglected, permitting the use of a one-dimensional analysis.

Situations are considered (see [28] for details) in which the surface is heated resistively. At low surface temperatures, the surface chemistry is sufficiently inactive. As the power is increased, however, the surface temperature becomes high enough to allow catalytic reaction that significantly raises the surface temperature. Once the catalyst is "lighted," the imposed power to the surface can be reduced or eliminated and the surface remains at the high combustion temperatures.

In a stagnation-flow field, scalar quantities (temperature and mass fractions) depend only on the distance from the surface and not on the radial position. The boundary-value problem to be solved together with the equation of state is [28-31]

Mixture continuity:

$$\frac{1}{\rho}\frac{\partial \rho}{\partial t} = -\frac{\partial u}{\partial x} - 2V - \frac{u}{\rho}\frac{\partial \rho}{\partial x} = 0 \tag{11}$$

Radial momentum:

$$\rho\frac{\partial V}{\partial t} = \frac{\partial}{\partial x}\left(\mu\frac{\partial V}{\partial x}\right) - \rho u\frac{\partial V}{\partial x} - \rho V^2 - \frac{1}{r}\frac{\partial p}{\partial r} = 0 \tag{12}$$

Thermal energy:

$$\rho c_p\frac{\partial T}{\partial t} = \frac{\partial}{\partial x}\left(\lambda\frac{\partial T}{\partial x}\right) - \rho c_p u\frac{\partial T}{\partial x} - \sum_{k=1}^{K_g}\left(c_{pk}\rho w_k V_k\frac{\partial T}{\partial x} + \dot{\omega}_k h_k\right) + S_q(x) = 0 \tag{13}$$

Species continuity:

$$\rho\frac{\partial w_k}{\partial t} = -\frac{\partial \rho w_k V_k}{\partial x} - \rho u\frac{\partial w_k}{\partial x} + M_k\dot{\omega}_k = 0 \quad \left(k=1,\ldots,K_g\right) \tag{14}$$

Surface species

$$\frac{dZ_k}{dt} = \frac{\dot{s}_k}{\Gamma} = 0 \tag{15}$$

In the governing equations the independent variables are the distance x normal to the disk surface, and the time t. The dependent variables are the axial velocity u, the radial velocity v which is scaled by the radius as $V=v/r$, the temperature T, the gas-phase species mass fractions w_k, and the surface species site fractions Z_k. The meaning of the other symbols are: ρ = mass density, c_p = mixture specific heat capacity, M_k = molecular mass of species k, h_k = specific enthalpy, μ = viscosity, λ = thermal conductivity, p = thermodynamic pressure, R = universal gas constant, V_k = diffusion velocities (including thermal diffusion), ω_k = chemical production rate due to gas phase reactions, s_k = chemical production rate of species due to surface reactions, K_g = number of gas phase species, K_s = number of surface species (not including bulk-phase species), Γ = surface site density. $(1/r)(dp/dr)$ in the radial momentum equation is an eigenvalue of the problem [32.33]. The details of the chemical reaction rate formulation can be found in the user's manuals for the *CHEMKIN* [34] and *SURFACE CHEMKIN* [23] software. Details of the transport property formulation can be found in the user's manual for the *TRANSPORT* [35] software.

Equation (15) states simply the fact that in steady state the surface composition does not change. In some sense it could be considered as a (possibly complex) boundary condition on the gas-phase system. However, it is considered part of the system of governing equations, because the surface composition is determined as part of the solution. The surface boundary condition becomes relatively complex in the presence of heterogeneous surface reactions. The gas-phase mass flux of each species to the surface j_k is balanced by the creation or depletion rate of that species by surface reactions, i. e.

$$j_k = \rho w_k V_k = \dot{s}_k \qquad \left(k = 1,\ldots,K_g\right). \tag{16}$$

The radial surface velocities V are specified by a no-slip boundary condition as $V = 0$. The surface temperature is determined from an energy balance that considers conductive, convective, and diffusive energy transport from the gas phase, radiation, chemical heat release, and resistive heating of the surface,

$$\lambda \frac{\partial T}{\partial x} - \sum_{k=1}^{K_g} \rho w_k V_k h_k = \sigma\varepsilon\left(T^4 - T_w^4\right) + \sum_{k=K_g+1}^{K_g+K_s} \dot{s}_k M_k h_k + \dot{P}. \tag{17}$$

Here, σ = Stefan-Boltzmann constant, ε = surface emissivity, and T_w = wall temperature to which the surface radiates. The term $\dot{P}$ represents an energy source (here resistance heating in the surface). At a height L above the surface, the boundary conditions correspond to a mixture of hydrogen and oxygen at room temperature and at a specified velocity.

The computational solution of the stagnation-flow problem is accomplished with the program *SPIN* [36], which, in turn, uses the *TWOPNT* [37] software that implements a Newton/Time-Step algorithm [38].

3.2.2. The flat-plate boundary layer

The flow field in the flat-plate boundary layer is shown schematically in Fig. 4. At a distance of $x=0$ at the bottom of a flat plate a uniform upward velocity is imposed. In addition, the inlet-gas composition and temperature are also independent of the distance y normal to the plate and the normal velocity component is zero. According to the experiments [26,27] a constant temperature is prescibed at the surface.
The mathematical description of a boundary layer over a flat plate is given in detail elsewhere in the literature [39,40]. For the planar configuration given in Fig. 4, the conservation equations can be written as

Momentum:

$$\rho u \frac{\partial u}{\partial x} + \frac{dp}{dx} = \rho u \frac{\partial}{\partial \psi}\left(\rho u \mu \frac{\partial u}{\partial \psi}\right) + \rho g \tag{18}$$

Thermal energy:

$$\rho u c_p \frac{\partial T}{\partial x} = \rho u \frac{\partial}{\partial \psi}\left(\rho u \lambda \frac{\partial T}{\partial \psi}\right) - \sum_{k=1}^{K_g} \dot{\omega}_k M_k h_k - \rho^2 u \sum_{k=1}^{K_g} c_{pk} w_k V_k \frac{\partial T}{\partial \psi} \tag{19}$$

Species:

$$\rho u \frac{\partial w_k}{\partial x} = M_k \dot{\omega}_k - \rho u \frac{\partial}{\partial \psi}\left(\rho w_k V_k\right) \qquad \left(k = 1,\ldots,K_g - 1\right) \tag{20}$$

where the symbols have the same meaning as in (11) - (15) and g = gravitational acceleration. The equation of state (6) and the surface species conservation (15) have to be added to this system. The independent variables are x, the distance along the plate surface, and $\psi = \int_0^y \rho u dy$, a density-weighted stream-function coordinate normal to the surface, where y is the physical space coordinate normal to the surface. The dependent variables in this parabolic differential equation system are p, ρ, u, T, w_k and Z_k.

After discretization of the spatial derivatives (central differences on a fixed grid of ψ), the resulting system of differential/algebraic equations in x is solved using the code *DASSL* developed by *Petzold* [41].

3.2.3. Physical chemistry of the problem

The gas-phase reaction mechanism is taken directly from modelling work on flame chemistry (see [28]). Its validity has been established through numerous studies of flames, shock-tubes, flow reactors and stirred reactors. In this work it is applied without modification.

A Pt surface reaction mechanism with associated rate expressions following the work of *Hellsing et al.* [42,43] is used. It accounts for dissociative adsorption of both H_2 and O_2, formation of adsorbed H_2O via adsorbed OH, and desorption of H_2O. This mechanism is based on OH LIF measurements and is similar to reaction schemes postulated by *Lin et al.* [44] and by *Schmidt et al.* [45]. In our mechanism, these reactions were supplemented with additional reactions for the adsorption of H, OH, O, and H_2O. The complete surface reaction mechanism, the used pre-exponential factors A, the activation energies E, and the sticking coefficients are given in Table 1 [28].

Table 1 Surface Reaction Mechanism of Hydrogen Oxidation (see [28] for details and references)

1. H_2/O_2 Adsorption/Desorption								A(cm,mol,s),S	E_a(kJ/mol)	
H_2	+	Pt(s)	=	H_2(s)				0.10	0.0	(sticking coefficient)
H_2(s)	+	Pt(s)	=	H(s)	+	H(s)		1.50E+23	17.8	(rate coefficient)
O_2	+	Pt(s)	=	O_2(s)				0.046	0.0	(sticking coefficient)
O_2(s)	+	Pt(s)	=	O(s)	+	O(s)		5.00E+24	0.0	(rate coefficient)
2. Surface Reactions										
H(s)	+	O(s)	=	OH(s)	+	Pt(s)		3.70E+21	19.3	(rate coefficient)
H(s)	+	OH(s)	=	H_2O(s)	+	Pt(s)		3.70E+21	0.0	(rate coefficient)
OH(s)	+	OH(s)	=	H_2O(s)	+	Pt(s)		3.70E+21	0.0	(rate coefficient)
3. Product Adsorption/Desorption										
H	+	Pt(s)	=	H(s)				1.00	0.0	(sticking coefficient)
O	+	Pt(s)	=	O(s)				1.00	0.0	(sticking coefficient)
H_2O	+	Pt(s)	=	H_2O(s)				0.75	0.0	(sticking coefficient)
OH	+	Pt(s)	=	H(s)				1.00	0.0	(sticking coefficient)

3.3. Results and discussion

3.3.1. Stagnation-flow field

The example considered here is an instationary hydrogen-oxygen stagnation-point flow to a platinum surface with constant heating of the foil [28]. In the experiments [18] a mixture of 25% H_2 and 75% O_2 at room temperature and at a total pressure of 100 mTorr (13.2 Pa) flows towards a resistively heated platinum foil. Based on measured flow rates and the gas inlet diameter, the inlet velocity is estimated to be 3,000 cm/s. The surface temperature and thus the ignition point is detected by means of the electrical current applied to the foil. The current is converted to a power per unit surface area taking into account the cross-sectional area of the foil and the resistance of platinum as a function of temperature. The energy balance at the surface requires estimating the radiative losses from the foil which, in turn, requires estimating the emissivity of the platinum (~0.1 for Pt in the ignited case, ~0.3 for oxidized Pt in the unignited case [46]).

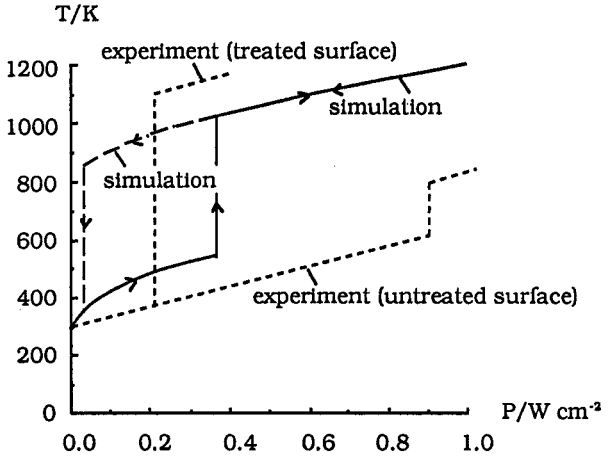

Figure 5. Ignition of 25% hydrogen- 75% oxygen mixtures on Pt at p=100 mTorr [28]

Figure 5 shows the result of a simulation [28] together with experimental curves [18] for an un-cleaned platinum foil and a platinum foil which has been treated by a series of ignitions. The larger temperature jump in the experiment might be caused by chemical reactions and heat release on the backside of the foil.

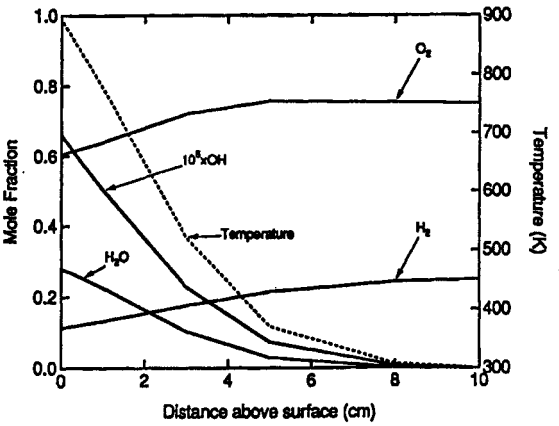

Figure 6. Temperature and mole fractions in the gas phase for a hydrogen-oxygen mixtures on Pt (P = 0.8 W cm^{-2}) after ignition (see [28])

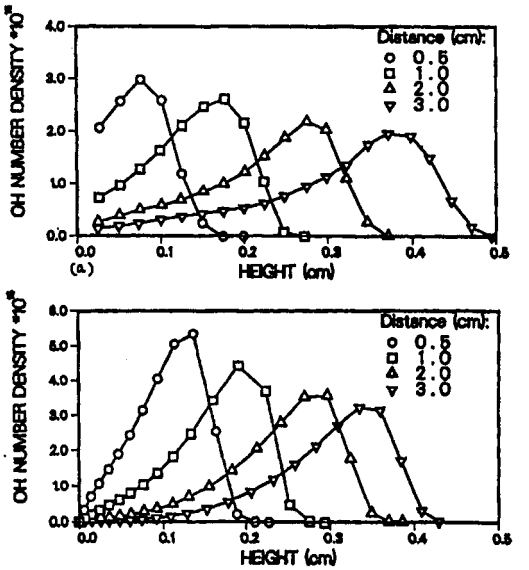

Figure 7. Stabilization of a hydrogen-air flame in a platinum flat plate boundary layer. Upper drawing: experiments; lower drawing: simulation (see [28] for details)

Figure 6 shows the predicted temperature and species profiles in the gas-phase above the platinum surface for an imposed power of 0.8 W cm^{-2}. The fact that the temperature and the water concentration are highest at the surface are clear indicators that catalytic combustion is occurring (in contrast to gas-phase combustion induced by a hot surface). The hydroxy radical is seen in low concentrations and is desorbed from the surface. Hydrogen- and oxygen atoms have very low concentrations (not shown in Fig. 6) and are adsorbed. A further indication of the catalytic behaviour is seen by omitting the surface chemistry in the simulation. In this case, the surface temperature is significantly lower, with its temperature supported only by the input power. The surface coverage consists mainly of O(s) before ignition and of free Pt(s) after ignition.

3.3.2. Flat-plate boundary layer

Reaction mechanisms which are based on elementary chemistry, should be equally applicable to different flow geometries and pressure ranges. As a test of their validity, we simulated experiments of *Cattolica and Schefer* [26,27] for a boundary-layer flow of hydrogen/air over a heated platinum surface at atmospheric-pressure. Predicted OH profiles and the measurements are shown in Fig. 7 [28].

Under these conditions combustion is mainly a gas-phase process. Primary evidence for this observation is that the peak OH-concentration is in the gas phase boundary layer. Furthermore, *Cattolica and Schefer* found that combustion occurs in presence of a (presumably non-catalytic) quartz surface, which is also confirmed by our simulations. As observed in the experiments, we also find that gradients in the OH profiles to the surface appear when a catalytic surface is used, showing that the surface is a sink for OH radicals.

The mixture considered is close to the flammability limit and calculations are very sensitive to small changes in the gas-phase reaction rate coefficients. Using the reported experimental flow conditions, the calculation predicted OH-profiles qualitatively different from the measurements. However, increasing the surface temperature to 1220 K (the reported temperature is 1170 K) produces the good agreement shown in Fig. 7, both in profile shape and peak magnitude. Given the high sensitivity to the surface temperature we believe that the observed OH profiles can be explained by inaccuracies in the measured surface temperature. Thus we conclude that the mechanisms satisfactorily reproduce the experimental results.

4. REFERENCES

[1] G. Dixon-Lewis, T. David, P.H. Gaskell, S. Fukutani, H. Jinno, J.A. Miller, R.J. Kee, M.D. Smooke, N. Peters, E. Effelsberg, J. Warnatz, and F. Behrendt, *20th Symp. (International) on Combustion*, 1893, The Combustion Institute, Pittsburgh, PA (1985).

[2] J. Warnatz, *18th Symp. (International) on Combustion*, 369, The Combustion Institute, Pittsburgh, PA (1981).

[3] M.D. Smooke, R.E. Mitchell, D.E. Keyes, *Combust.Sci. Technol. 67*, 85 (1989).

[4] J. Warnatz, U. Maas, Calculation of the Detailed Structure of Premixed and Non-Premixed Flame Fronts and Some Applications, IMACS Transactions on Scientific Computing '88, in: *Numerical and Applied Mathematics*, p. 151-157, W.F. Ames (ed.), J.C Baltzer AG, Scientific Publishing Co., (1989)
[5] W. A. Sirigiano, *Prog. Energy Combust. Sci. 9*, 291 (1983)
[6] A. Makino, C. K. Law, *Combust. and Flame 73*, 331 (1988)
[7] M. Mavid, S. K. Aggarwal, *Combust. Sci. and Tech. 65* (1989)
[8] C. K. Law, *Prog. Energy Combust. Sci. 3*, 137 (1977)
[9] C. K. Law, *Prog. Energy and Combust. Sci. 10*, 295 (1984)
[10] P. Stapf, C. Chevalier, U. Maas, J. Warnatz and H.A. Dwyer, *Proc. 13th ICDERS*, Nagoya (1991)
[11] P. Stapf, U. Maas, J. Warnatz, *Proc. 7th TECFLAM Seminar*, ISBN 3-926751-12-6
[12] P. Stapf, U. Maas, J. Warnatz, publication in preparation
[13] R. C. Reid, J. M. Prausnitz, B. E. Poling, *The Properties of Gases and Liquids*, McGraw-Hill (1986)
[14] J. O. Hirschfelder, C. F. Curtiss, R. B. Bird, *Molecular Theory of Gases and Liquids*, John Wiley & Sons, Inc., New York, 2nd printing (1964)
[15] J. O. Hirschfelder, C. F. Curtiss, *3rd. Symp. Comb. Flame and Explosion Phenomena*, pp. 121-127, Williams and Wilkins Cp., Baltimore (1949)
[16] H. Davy, "Some New Experiments and Observations on the Combustion of Gaseous Mixtures", in: *The Collected Works of Sir Humphrey Davy* (J. Davy ed.), Vol. 6, Smith, Elder, and Co., Cornhill, London (1840)
[17] I. Langmuir, *Trans. Faraday Soc.* 17, 621 (1922)
[18] S. Ljungström, B. Kasemo, A. Rosen, and T. Wahnström, E. Fridell, *Surface Sci. 216*, 63-92 (1989)
[19] D. S. Y. Hsu, M. A. Hoffbauer, M. C. Lin, *Surf. Sci. 184*, 25 (1987)
[20] L. D. Pfefferle, W. C. Pfefferle, *Catal. Rev. - Sci. Eng. 29*, 219-267 (1987)
[21] X. Song, W. R. Williams, L. D. Schmidt, R. Aris, *Twenty-Third Symposium (International) on Combustion*, p. 1129. The Combustion Institute, Pittsburgh, PA (1991)
[22] M. E. Coltrin, R. J. Kee, and F. M. Rupley, "Surface Chemkin: A General Formalism and Software for Analyzing Heterogeneous Chemical Kinetics at a Gas-Surface Interface," *Intl. J. Chem. Kin.* (1991), to appear
[23] M. E. Coltrin, R. J. Kee, and F. M. Rupley, "Surface Chemkin (Version 3.7): A Fortran Package for Analyzing Heterogenous Chemical Kinetics at a Solid-Surface-Gas-Phase Interface," Sandia National Laboratories Report, *SAND90-8003* (1990)
[24] M. D. Allendorf and R. J. Kee, *J. Electrochem. Soc. 139*, 841 (1991)
[25] R. E. Mitchell, R. J. Kee, P. Glarborg, and M. E. Coltrin, *Twenty-Third Symposium (International) on Combustion*, p. 1169. The Combustion Institute, Pittsburgh, PA (1990)
[26] R. J. Cattolica, R. W. Schefer, *Comb. Sci. Technol. 30*, 205-212 (1983)
[27] R. J. Cattolica, R. W. Schefer, *Nineteenth Symposium (International) on Combustion*, pp. 311-318, The Combustion Institute, Pittsburgh, PA (1982)
[28] J. Warnatz, M.D. Allendorf, R.J. Kee, M.D. Coltrin, submitted to Combustion and Flame
[29] R. J. Kee, J. A. Miller, G. H. Evans, and G. Dixon-Lewis, *Twenty-Second Symposium (International) on Combustion*, pp. 1479-1494. The Combustion Institute, Pittsburgh, PA (1988)
[30] G. Evans and R. Greif, *J. Heat Trans. ASME 109*, 928 (1987)
[31] M. E. Coltrin, R. J. Kee, and G. H. Evans, *J. Electrochem. Soc. 136*, 819 (1989)
[32] G. Stahl, J. Warnatz, *Combustion and Flame 85*, 285 (1991)
[33] G. Dixon-Lewis, S. Fukutani, J. A. Miller, N. Peters, J. Warnatz et al., Twentieth Symposium (International) on Combustion, p. 1893. The Combustion Institute, Pittsburgh (1985)
[34] R. J. Kee, F. M. Rupley, and J. A. Miller, "CHEMKIN-II: A Fortran Chemical Kinetics Package for the Analysis of Gas-Phase Chemical Kinetics," Sandia National Laboratories Report *SAND89-8009* (1989)
[35] R. J. Kee, G. Dixon-Lewis, J. Warnatz, M. E. Coltrin, and J. A. Miller, "A Fortran Computer Code Package for the Evaluation of Gas-Phase Multi-component Transport Properties," Sandia National Laboratories Report *SAND86-8246* (1986)
[36] M. E. Coltrin, R. J. Kee, G. H. Evans, E. Meeks, F. M. Rupley, and J. F. Grcar, "SPIN: A Fortran Program for Modelling One-Dimensional Rotating Disk/ Stagnation-Flow Chemical Vapour Deposition Reactors," Sandia National Laboratories Report *SAND91-8003* (1991)
[37] J. F. Grcar, "The TWOPNT Program for Boundary Value Problems," Sandia National Laboratories Report *SAND91-8230* (1991)
[38] J. F. Grcar, R. J. Kee, M. D. Smooke, J. A. Miller, *Twenty-First Symposium (International) on Combustion*, p. 1773. The Combustion Institute, Pittsburgh, PA (1986)
[39] M. E. Coltrin, R. J. Kee, J. A. Miller, *J. Electrochem. Soc. 131*, 425 (1984)
[40] M. E. Coltrin, R. J. Kee, J. A. Miller, *J. Electrochem. Soc. 133*, 1206 (1986)
[41] L. R. Petzold, "A Description of DASSL: A Differential/Algebraic System Solver," Sandia National Laboratories Report *SAND82-8637* (1982)
[42] B. Hellsing, B. Kasemo, S. Ljungström, A. Rosen, and T. Wahnström, *Surface Sci. 189/190*, 851 - 860 (1987)
[43] B. Hellsing and B. Kasemo, *Chemical Phys. Letters 148*, 465-471 (1988)
[44] D. H. Hsu, M. A. Hoffbauer, M. C. Lin, *Surf. Sci. 184*, 25 (1987)
[45] W. R. Williams, C. M. Marks, L. D. Schmidt, Steps in the Reaction $H_2 + O_2 = H_2O$ on Pt: OH Desorption at High Temperature (to be submitted)
[46] *Handbook of Chemistry and Physics*, 63rd Ed., p. E-386 (1982)